

## Research Article

# Feature Preserving Filling of Holes on Point Sampled Surfaces Based on Tensor Voting

Hongbin Lin , Jieyun Chen, Yaru Zhang, Wei Wang, and Deming Kong 

*School of Electrical Engineering, Yanshan University, Qinhuangdao 066004, China*

Correspondence should be addressed to Hongbin Lin; honphin@ysu.edu.cn

Received 2 March 2018; Revised 22 May 2018; Accepted 24 June 2018; Published 14 August 2018

Academic Editor: Mariko Nakano-Miyatake

Copyright © 2018 Hongbin Lin et al. This is an open access article distributed under the Creative Commons Attribution License, which permits unrestricted use, distribution, and reproduction in any medium, provided the original work is properly cited.

This paper presents a novel hole filling method for the scattered point sampled surfaces, particularly for recovering the missing points at featured curves or corners. Firstly, a tensor voting based multicriterion is proposed to identify the hole boundary points; accordingly, the holes on point sampled surface are classified into featured holes and nonfeatured holes. Secondly, a novel spline curve guided tensor voting mechanism is proposed and used in inference of missing feature points. Thirdly, the featured holes are split into nonfeatured holes using local projection. Then, a plane guided tensor voting mechanism is proposed to recover the missing surface points. Experimental results validate the effectiveness and accuracy of proposed methods in filling holes on point sampled surface including the sharp features.

## 1. Introduction

Point sampled surfaces are sets of data points and can be acquired through three-coordinate measuring equipment. It is an important data source in reverse engineering and is widely used in many fields, such as industrial measurement, restoration of cultural relics, fashion design, and medical research [1]. Point cloud or point sampled surface has become an important form of digital media. However, for many reasons, such as occlusion, the damaging of original models, or limitation of scanners, the point cloud model of the original object may be incomplete and form different types of holes. These holes influence many subsequent operations, such as model rebuilding, rapid prototyping, and finite element analysis. Therefore it is necessary to fill and repair them in a reasonable manner.

Although several hole filling methods have been proposed, it is worthy pointing out that most of them are suitable for some holes located on smooth regions (without missing feature points). However, an ideal hole filling algorithm should be able to deal with the complex holes including an island or one with missing sharp features. In addition, it should be able to preserve the geometric features of the original object. Due to the diversity and complexity of the holes, none of existing methods work for all holes.

In this paper, we focus on the different holes that may have some locating on feature regions and present a novel feature preserving hole filling algorithm. Firstly, we determine the hole boundary and the incomplete feature curves and categorize the holes on point sampled surface into two types, the featured holes and the nonfeatured holes. Then, spline guided tensor voting was proposed and used to restore the missing part of feature curves. And these reconstructed feature curves split the original hole into simple subholes. Finally, all the nonfeatured holes were filled by the plane guided tensor voting. The main contributions of our algorithm can be summarized as follows:

(1) A multicriterion is developed in order to improve the reliability of hole boundary point identification. In the construction, the tensor voting based hole boundary identification criterion is proposed and combined with half disk criterion and maximum angle criterion.

(2) A spline curve guided tensor voting mechanism is proposed and used in inference of missing feature points, which gets rid of either the oversmoothed reconstruction of direct spline curve fitting or the inefficiency of traditional Single Sub-Voxel C Marching.

(3) A plane guided tensor voting mechanism is proposed and used in inference of surface points, to improve the accuracy and efficiency of the algorithm.

The rest of this paper is organized as follows. The related work is briefly reviewed in Section 2. Section 3 presents the outline of our method. Hole boundary point identification and hole classification methods are proposed in Section 4. Section 5 presents our feature point filling method. Our sub-hole filling method is described in Section 6. Section 7 presents the experimental results. And, in the last section, the limitations of our method and proposals for future research are indicated.

## 2. Related Work

Many holes filling algorithms have been proposed in recent years. In general, existing algorithms can be categorized into two types: mesh-based methods and point-based methods. At present, a large portion of methods is based on mesh models, which make use of topological information. Topological connection make the hole boundary identification and geometrical estimation easy; meanwhile, the topological reconstruction of incomplete point itself is still challenging. On the other hand, the point model is often obtained by scanning equipment and is easily affected by noise and not being able to deal directly with it. Thus, the geometrical estimation as well as hole filling directly on point sampled surface is more challenging than that on meshed surface.

*2.1. Mesh-Based Methods.* Mesh-based methods often fill holes locally with the rest of the surface unchanged. Liepa [2] used refinement and fairing to refine the obtained patch mesh, so that the triangle density coincide with that of the surrounding mesh. This method was further used by Attene [3]. Pernot et al. [4] filled holes by minimizing the curvature variant between the surrounding and inserted meshes.

Another class of mesh-based methods is the volumetric based methods in which the mesh model is firstly converted into a volume representation. During the repairing process, the generation of a signed volume is the key step. Davis et al. [5] defined a signed distance function in the vicinity of the observed surface and applied a diffusion process to extend this function until its zero set bridged all holes. Ju [6] employed a space-efficient octree grid and generated blobby surfaces by recording Hermite data, to reproduce the sharp features.

NURBS curves and surfaces are also a kind of repair tools for the holes located on smooth regions of a model. For these types of methods, one needs to choose weights and solve a large system of equations to compute the knot vectors. Piegl and Tiller [7] used NURBS patches to fill an n-sided region. Besides, Xu et al. [8] and Park et al. [9] proposed the surface filling method based on PDEs independently. Zhao et al. [10] proposed the mesh repair algorithm based on the Poisson equation.

*2.2. Point-Based Method.* The point model are often obtained by scanning equipment, and is easily affected by noise and not being able to deal directly with it. Thus, the geometrical estimation as well as hole filling directly on point sampled surface is more challenging than that on meshed surface. In this field, Sharf et al. [11] proposed a context-based method, in which, the characteristics of the given surface were analyzed,

and the holes were iteratively filled by copying patches from valid regions of the given surface. Pavel and Bert [12] described a method for identifying and filling holes on point sampled surfaces; they fitted an algebraic surface patch to the neighborhood and sample auxiliary points. Chen et al. [13] proposed an algorithm based on the average error and average curvature to fill up hole areas of point sampled surfaces.

Above-mentioned algorithms including the mesh-based methods and the point-based methods are able to fill certain holes precisely, while when the hole exhibits complex shapes, e.g., containing the sharp corners or edges of original model, the filling quality declines significantly. In response to this issue, a sensible strategy is to split the original complex hole into small subholes according to a feature analysis and then fill those small holes, respectively. The key step is to reconstruct missing parts of the feature curves in advance. Jun [14] presented a piecewise hole filling algorithm for complex holes. This algorithm incrementally splits a complex hole into small subholes with respect to the shape of the holes boundary and then fills 104 simple holes each with planar triangulation method. Li et al. [15] proposed a feature preserving mesh holes filling algorithm, which used a polynomial blending curve to construct the missing parts of the feature curves and used the Bézier-Lagrange hybrid patch to fill each subhole. Similarly, Wang et al. [16] used Gaussian mapping and convex/concave analysis to produce missing feature curves and filled each subhole by a modified advancing front method individually. Lin and Wang [17] presented a tensor voting based hole filling method for the scattered point cloud, particularly for recovering the missing points at featured curves or corners.

It is worth mentioning that these methods are suitable for mesh model rather than point models. Feature preserving filling of complex holes directly on point sampled surface is still an issue. This paper extended the tensor voting based hole filling method proposed in [17] through novel feature curves reconstruction using spline guided tensor voting and recovering of nonfeatured points using plane guided tensor voting.

## 3. Algorithm Overview

In this paper, we make use of the robust structure inference ability of tensor voting technique to identify the hole boundary points and infer the missing curve points and the surface points. Fundamental usage and further application of tensor voting technique can be found in [18–23].

The procedure of the proposed hole filling method is illustrated in Figure 1. Firstly, the multicriterion hole boundary point identification method is proposed based on tensor voting. Secondly, the feature points are identified using tensor voting; refer to [24]. Then, holes are classified into featured holes and nonfeatured holes by checking whether feature points are contained in the hole boundary points sets. Featured holes are firstly treated with feature sets matching [16], and then spline guided tensor voting is proposed and used in feature curves reconstruction. Finally, the featured holes are split into nonfeatured hole through local projection, and the nonfeatured holes are filled by proposed plane guided tensor

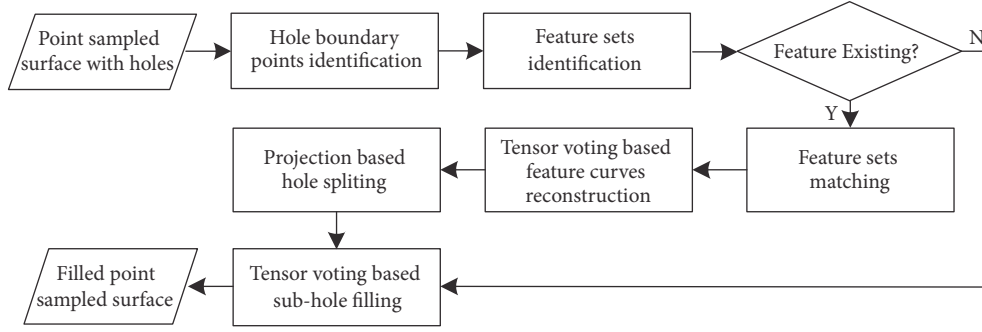


FIGURE 1: Overview of the holes filling method.

TABLE 1: The classification of points.

Decision vector	Point type
$\eta_1 \gg \eta_2 \approx \eta_3$	Inner point
$\eta_1 \approx \eta_2 \gg \eta_3$	Curve point
$\eta_1 \approx \eta_2 \approx \eta_3$	Corner point or noise
$\eta_1 \gg \eta_2 \gg \eta_3$	Hole boundary point

voting. Due to this split and inference strategy, structures as well as sharp features of original model could be preserved effectively.

## 4. Hole Classification

**4.1. Hole Boundary Point Identification.** Identification of hole boundary points can be challenging due to the deficiency of topological connection information in point sampled surface. Hence, a multicriterion hole boundary point identification method is proposed in this section based on tensor voting.

Let  $\mathbf{P}$  be a point sampled surface,  $\mathbf{p}(x_0, y_0, z_0)$  be a 3D point in  $\mathbf{P}$ , and  $\mathbf{p}_1, \mathbf{p}_2, \dots, \mathbf{p}_k$  are neighbors of  $\mathbf{p}$ .  $\mathbf{n}(n_x, n_y, n_z)$  is the normal at  $\mathbf{p}$ , as illustrated in Figure 2.

The local tangent plane  $\Pi$  at  $\mathbf{p}$  can be expressed as  $n_x x + n_y y + n_z z - (n_x x_0 + n_y y_0 + n_z z_0) = 0$ . Let  $\mathbf{p}'_j$ ,  $j = 1, 2, \dots, k$ , be the projected neighbors on  $\Pi$  along normal  $\mathbf{n}$ .

Suppose  $\mathbf{T} \in R^{3 \times 3}$  is voted tensor at point  $\mathbf{p}$  and  $\mathbf{e}_1, \mathbf{e}_2, \mathbf{e}_3$  and  $\lambda_1, \lambda_2, \lambda_3$  (where  $\lambda_1 \geq \lambda_2 \geq \lambda_3 \geq 0$ ) are the eigen vectors and corresponding eigenvalues of  $\mathbf{T}$ . Let us construct the tensor voting decision vector  $\eta = [\eta_1, \eta_2, \eta_3]^T$  by

$$\begin{aligned} \eta_1 &= \frac{\sqrt{\lambda_1}}{\sqrt{\lambda_1} + \sqrt{\lambda_2} + \sqrt{\lambda_3}}, \\ \eta_2 &= \frac{\sqrt{\lambda_2}}{\sqrt{\lambda_1} + \sqrt{\lambda_2} + \sqrt{\lambda_3}}, \\ \eta_3 &= \frac{\sqrt{\lambda_3}}{\sqrt{\lambda_1} + \sqrt{\lambda_2} + \sqrt{\lambda_3}}. \end{aligned} \quad (1)$$

According to tensor voting theory, the relationship between point type and constructed tensor voting decision vector can be concluded as in Table 1.

Let us construct our tensor voting criterion  $f_T(p, k)$  by

$$f_T(\mathbf{p}, k) = 9(\eta_1 - \eta_2)(\eta_2 - \eta_3), \quad (2)$$

where  $\mathbf{p}$  is the point to be analyzed and  $k$  is the neighboring number.

Suppose  $f_\theta(\mathbf{p}, k)$  is the hole boundary identifying function composed of the half disk criterion, defined as follows [25]:

$$f_\theta(\mathbf{p}, k) = \frac{\theta_{max} - 2\pi/k}{\pi - 2\pi/k}, \quad (3)$$

where  $\theta_{max}$  is the maximum separated angle.

Suppose  $f_g(\mathbf{p}, k)$  is the hole boundary identifying function composed of the half disk criterion, defined as follows [25]:

$$f_g(\mathbf{p}, k) = \frac{3\pi \|\mathbf{g} - \mathbf{p}\|}{4r}, \quad (4)$$

where  $\mathbf{g} = (1/k) \sum_{i=1}^k \mathbf{p}'_i$  is the gravity center of projected neighbors and  $r = (1/k) \sum_{i=1}^k \|\mathbf{p} - \mathbf{p}'_i\|$  is the averaged distance between projected neighbors and point  $\mathbf{p}$ .

Finally, we construct our multicriterion hole boundary point identification function  $F(\mathbf{p}, k)$  by normalizing and weighting  $f_\theta(\mathbf{p}, k)$ ,  $f_g(\mathbf{p}, k)$  and proposed  $f_T(\mathbf{p}, k)$  by

$$\begin{aligned} F(\mathbf{p}, k) &= \omega_\theta G(f_\theta(\mathbf{p}, k)) + \omega_g G(f_g(\mathbf{p}, k)) \\ &\quad + \omega_T G(f_T(\mathbf{p}, k)), \end{aligned} \quad (5)$$

where  $G(x) = (x - x_{min}) / (x_{max} - x_{min})$  is the normalization function,  $\omega_\theta, \omega_g$ , and  $\omega_T$  (fulfilling  $\omega_\theta + \omega_g + \omega_T = 1$ ) are weights of the three identifying criterion, and  $x_{min}$  and  $x_{max}$  are the minimum and maximum value of the variable.

Figure 3 shows identifying results of hole boundary points using different methods, which reveals that the proposed multicriterion function is able to identify the hole boundary points reliably.

**4.2. Hole Classification.** Considering the variety of holes and the efficiency of holes filling methods we simply classify the holes based on their feature. In recent years some methods of hole classification have been presented, and the general

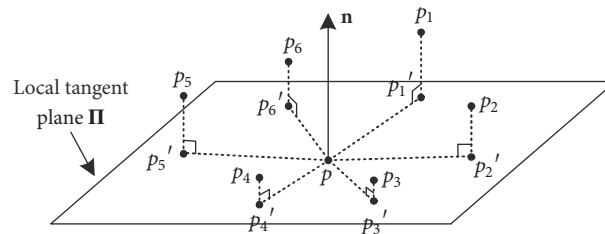


FIGURE 2: Illustration of neighboring projection.

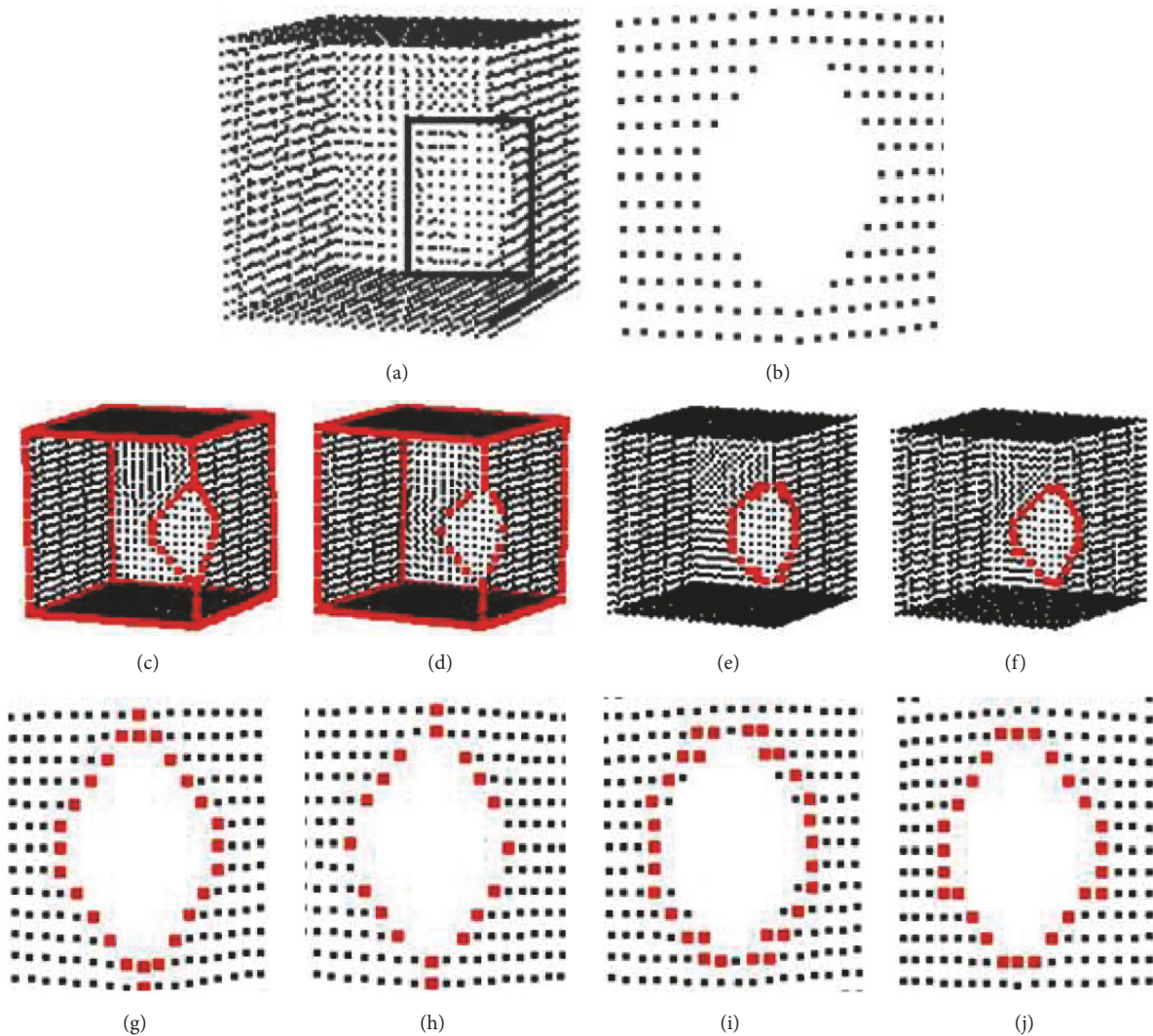


FIGURE 3: Hole boundary points identifying results: (a) original point cloud, (b) partial enlarged detail of hole region, (c) identified result by maximum angle criterion, (d) identified result by half disk criterion, (e) identified result by tensor voting criterion, (f) identified result by proposed multicriterion method, (g) partial enlarged detail of identified result by maximum angle criterion, (h) partial enlarged detail of identified result by half disk criterion, (i) partial enlarged detail of identified result by tensor voting criterion, and (j) partial enlarged detail of identified result by proposed multicriterion method.

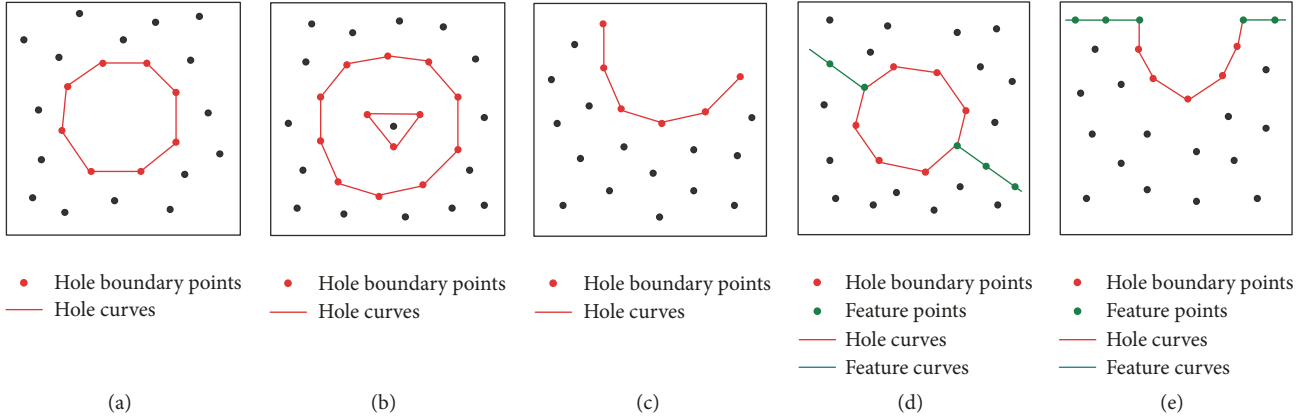


FIGURE 4: The basic hole classification: (a) single-close hole, (b) island-close hole, (c) unclosed hole, (d) featured closed hole, and (e) featured unclosed hole.

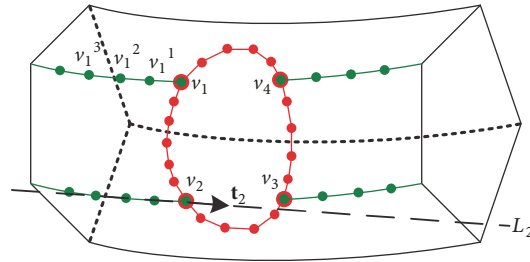


FIGURE 5: Illustration of the hole with missing feature.

method are showed in [26]. This paper reclassifies the holes by checking whether the feature points are contained in the hole boundary point sets. Accordingly, all holes on point sampled surfaces are classified into featured holes, as shown in Figures 4(a), 4(b), and 4(c) or nonfeatured holes as shown in Figures 4(d) and 4(e).

## 5. Feature Curve Reconstruction

In order to acquire satisfactory results in filling of complex holes (with missing sharp features), a reasonable method is to split the complex hole region combining the neighboring points into nonfeatured ones. In fact, multiple choices can be made for segmentation of the neighboring points. An effective way is the feature based region segmentation. Hence, reconstruction of feature curve and inference of curve structure within the hole region become the key operation.

For inference of missing curve structure, a straight way is fitting or interpolating of the neighboring feature points. Unfortunately, this type of operation often achieves over-smoothed curve structure, leading to distortion in complex hole filling. Another substitution is the robust machine learning method, such as Single Sub-Voxel C march [27], which is highly related on tensor voting and Marching Cubes. This type of methods tends to repair the missing points accurately with feature preserving. But, the filling-and-judge strategy of Single Sub-Voxel C march restricts its potential efficiency, preventing its further application. Thus, this section presents

a novel curve structure inference method, benefiting both from spline fitting and tensor voting.

Firstly, feature sets are matched using tangent projection [16]. As shown in Figure 5, points  $v_1$  and  $v_4$  are matched. Meanwhile, points  $v_2$  and  $v_3$  are also matched.

Afterwards, a new spline guided tensor voting strategy is proposed to infer the missing feature points, as illustrated in Figure 6.

Suppose  $p_1, p_2, \dots$  is the matched featured points and  $L$  is the fitted spline curve.  $o$  is a point on  $L$ ,  $u$  and  $v$  span the normal plane of  $L$  at  $o$ , and  $\omega$  is the normal of plane  $uv$ .

$$\begin{aligned} x &= F_x(t), \\ y &= F_y(t), \\ z &= F_z(t), \end{aligned} \quad (6)$$

Since  $L$  is the approximated feature curve, the real feature point must locate on the normal plane of  $L$  and receives local maximum plate tensor saliency (most probably being a curve point). Thus, we construct our local coordinate system  $uvw$  as shown in Figure 6 and place four imagined points  $q_1, q_2, q_3, q_4$  on  $uv$  around the circle centered at  $o$ , with radius  $r$ . The imagined points receive and accumulate tensor tokens voted from neighboring matched featured points  $p_1, p_2, \dots$ . Denote the tensor token at the four imaginary points by  $\mathbf{T}_1, \mathbf{T}_2, \mathbf{T}_3$ , and  $\mathbf{T}_4$  independently. Similarly, denote the plate saliency at the four imaginary points by  $s_1, s_2, s_3$ , and  $s_4$  independently. According to tensor voting theory, the real feature point holds

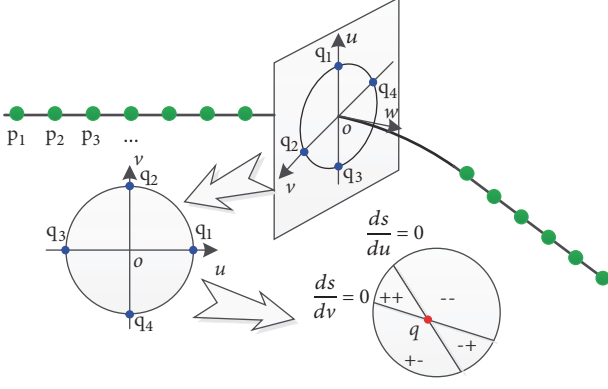


FIGURE 6: Illustration of the feature curve reconstruction.

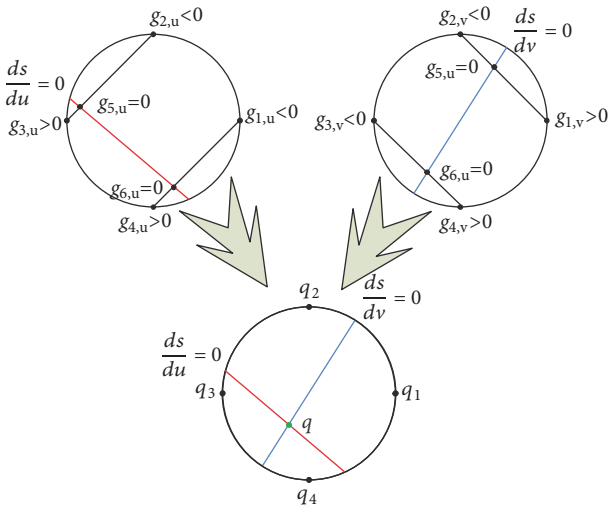


FIGURE 7: Illustration of proposed feature point estimation.

the local maximum plate saliency on plane  $uv$ , which means  $ds/du = ds/dv = 0$ , where  $s$  is the plate saliency of points on plane  $uv$ . Hence, the real feature point can be computed through interpolate of derivation of  $s_1, s_2, s_3$ , and  $s_4$ .

Mechanism of the proposed feature point estimation method is illustrated in Figure 7. Suppose  $g_{i,u} = ds_i/du$ ,  $g_{i,v} = ds_i/dv$ , where  $i, j = 1, 2, 3, 4$ . Since  $g_{2,u} < 0$  and  $g_{3,u} > 0$ , hence a point  $g_{5,u} = 0$  can be estimated by linear interpolation of  $g_{2,u}$  and  $g_{3,u}$ . Similarly,  $g_{6,u} = 0$  can also be estimated. Thus, the points on the line connecting  $g_{5,u}$  and  $g_{6,u}$  are considered to hold  $ds/du = 0$ . Similarly, another line with  $ds/dv = 0$  can also be estimated. And the feature point located on plane  $uv$  can be estimated by intersecting the two lines. In fact, the distribution of  $g_{i,u}$  and  $g_{i,v}$  on  $uv$  can be rather complicated, and the readers can refer to the Marching Cube type algorithms.

## 6. Subhole Filling

After feature curves reconstruction, the complex holes combining with their neighbors can be split into simple ones. For this, we constructed a local projection plane through gravity

TABLE 2: The number of distribution points.

Interval	$(0, d/2]$	$(d/2, d]$	$(d, 3d/2]$	$(3d/2, 2d]$	...
Count	0	1	2	3	...

center and averaged normal of hole boundary points. And then project the neighboring points and feature points on to the projection plane and segment the neighbor points by their relationship with the projected feature curve. Thus, the hole region and the neighboring points can be split into simple ones, as shown in Figure 8.

In order to fill the nonfeatured simple holes, this section proposed a plane guide tensor voting method as follows.

*Step 1.* Project all hole boundary points onto a local projection plane defined by gravity center and averaged normal of hole boundary points, as shown in Figure 9(a). In fact, the gravity center  $\bar{\mathbf{p}}$  of the hole and the averaged normal  $\bar{\mathbf{n}}$  of the projection plane can be computed by

$$\bar{\mathbf{p}} = \frac{1}{l} \sum_{j=1}^l \mathbf{p}_j = [x_0, y_0, z_0]^T, \quad (7)$$

$$\bar{\mathbf{n}} = \frac{1}{l} \sum_{j=1}^l \mathbf{n}_j = [n_x, n_y, n_z]^T, \quad (8)$$

where  $\mathbf{p}_j$  is the  $j$ th hole boundary point,  $\mathbf{n}_j$  is the normal of the  $\mathbf{p}_j$ . The projection plane defined by  $\bar{\mathbf{p}}$  and  $\bar{\mathbf{n}}$  can be expressed as follows:

$$\begin{bmatrix} x'_j \\ y'_j \\ z'_j \end{bmatrix} = \begin{bmatrix} x_j \\ y_j \\ z_j \end{bmatrix} - k_j \begin{bmatrix} n_x \\ n_y \\ n_z \end{bmatrix}, \quad (9)$$

where

$$k_j = \frac{n_x(x_j - x_0) + n_y(y_j - y_0) + n_z(z_j - z_0)}{n_x^2 + n_y^2 + n_z^2}. \quad (10)$$

*Step 2.* Distribute the distribution points on hole projection plane evenly, as shown in Figure 9(b). Denote the distance between  $\mathbf{p}'_j$  and  $\bar{\mathbf{p}}$  by  $d_j$ . Suppose the average distance between neighboring points within the original point sampled surface is  $d$ ; then distribute the distribution points with regular distances as shown in Table 2.

The coordinates of each distribution point can be precisely computed. As shown in Figure 9(b), the coordinates of distribution points  $\mathbf{p}'_{1a}$  and  $\mathbf{p}'_{1b}$  between  $\mathbf{p}'_1$  and  $\bar{\mathbf{p}}$  can be computed by

$$\begin{bmatrix} x'_{1a} \\ y'_{1a} \\ z'_{1a} \end{bmatrix} = \begin{bmatrix} x'_1 \\ y'_1 \\ z'_1 \end{bmatrix} + \frac{d}{3d_1} \begin{bmatrix} (x_0 - x'_1) \\ (y_0 - y'_1) \\ (z_0 - z'_1) \end{bmatrix}, \quad (11)$$

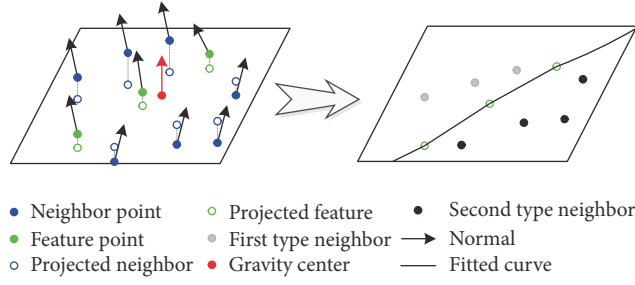


FIGURE 8: Illustration of holes filling without missing feature.

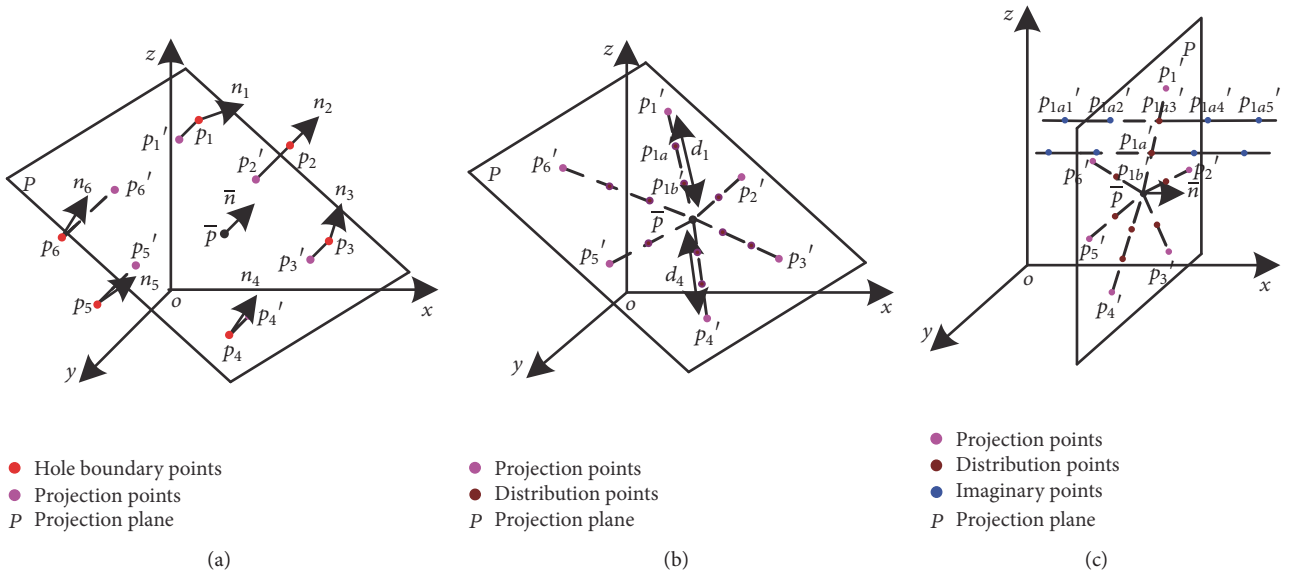


FIGURE 9: Illustration of holes filling without missing feature: (a) hole boundary projection, (b) distribution of distribution points, and (c) distribution of imaginary points.

and

$$\begin{bmatrix} x'_{1b} \\ y'_{1b} \\ z'_{1b} \end{bmatrix} = \begin{bmatrix} x'_1 \\ y'_1 \\ z'_1 \end{bmatrix} + \frac{2d}{3a_1} \begin{bmatrix} (x_0 - x'_1) \\ (y_0 - y'_1) \\ (z_0 - z'_1) \end{bmatrix}. \quad (12)$$

**Step 3.** Distribute evenly the imaginary points along the normal of the hole projection plane, and each surface saliencies of the imaginary points is accurately computed. As shown in Figure 9(c), the point set  $\mathbf{p}'_{1a1}, \mathbf{p}'_{1a2}, \dots, \mathbf{p}'_{1a7}$ , for example, is the imaginary points of the distribution point  $\mathbf{p}'_{1a1}$  along the normal  $\bar{\mathbf{n}}$ , and the spacing of two consecutive imaginary points is the original point cloud density  $d$ . The coordinates of imaginary point  $\mathbf{p}'_{1ak}$ ,  $1 \leq k \leq 7$ , can be computed as follows:

$$\begin{bmatrix} x'_{1ai} \\ y'_{1ai} \\ z'_{1ai} \end{bmatrix} = \begin{bmatrix} x'_{1a} \\ y'_{1a} \\ z'_{1a} \end{bmatrix} + (i-4)d \begin{bmatrix} n_x \\ n_y \\ n_z \end{bmatrix}, \quad (i = 1, 2, \dots, 7). \quad (13)$$

After determining the coordinates of imaginary points, their refined tensor tokens are required by dense tensor voting using existing points belonging to the same areas and decomposed to compute the surface saliencies.

**Step 4.** In order to further accurately calculate the filling point coordinates, two-order polynomial method fit method is put forward to estimate the extreme of surface saliencies.

Suppose the set of imaginary points  $\mathbf{p}'_{1a1}, \mathbf{p}'_{1a2}, \dots, \mathbf{p}'_{1a7}$  corresponding surface saliencies, respectively, is  $s_{1a1}, s_{1a2}, \dots, s_{1a7}$ . We firstly construct the 2D local coordinate system where the normal  $\bar{\mathbf{n}}$  corresponds to horizontal axle and the surface saliency corresponds to vertical axle, as shown in Figure 10, where  $b$  is the vertical distance from the imaginary point and the projection plane, and its sign is decided by their relative location. Then, the coefficients of a quadratic curve equation are estimated. The extreme of surface saliency is computed, when  $b' = -B/2A$ .

$$y = Ax^2 + Bx + C. \quad (14)$$

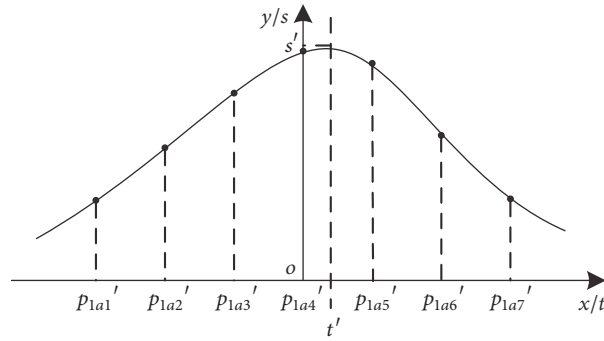


FIGURE 10: Illustration of the two-order polynomial method fit method.

TABLE 3: The distances from repair points to the original surface.

type	Hole Maximum(mm)			Average(mm)		
	Davis et al.	Centin et al.	Our method	Davis et al.	Centin et al.	Our method
I	0.19	0.00	0.00 ( $\sigma = 0.3$ )	0.14	0.00	0.00 ( $\sigma = 0.3$ )
II	0.21	0.07	0.15 ( $\sigma = 0.2$ )	0.04	0.03	0.04 ( $\sigma = 0.2$ )
III	0.33	0.87	0.01 ( $\sigma = 0.3$ )	0.05	0.60	0.00 ( $\sigma = 0.3$ )
IV	0.52	0.96	0.25 ( $\sigma = 0.3$ )	0.06	0.43	0.03 ( $\sigma = 0.3$ )
V	1.10	2.20	0.14 ( $\sigma = 0.2$ )	0.13	0.88	0.02 ( $\sigma = 0.2$ )

## 7. Experimental Results

This section performs our feature preserving holes filling experiments, which is coded with C++, running on Visual Studio 2010 software and Windows systems. In order to examine the performances of the algorithm on filling four types of holes (holes on plane, smoothed surface, with missing sharp curve, with missing corner), the Fandisk model was selected as the fundamental model for its possession of all these features. In our experiments, the techniques by Davis et al. [5] and by Centin et al. [28] were also used to fill the same holes for comparison. In order to better observe the experimental results, we demonstrate the meshed Fandisk models and hole areas.

**7.1. Filling of Simple Holes.** In order to examine the performances of the algorithm on filling simple holes, holes on plane (Hole I) and smooth surface (Hole II) are artificially generated and then filled by [5, 28] and proposed method.

As shown in Figure 11, Davis yields biased estimation for missing plane points, Centin's methods and proposed method achieve almost flat recovery without error, and numerical static error can be found in Table 3. This type of hole can also be ideally filled by plane extension for simplicity.

As shown in Figure 12, Centin's method yields ideal smoothed recovery of missing points on surface; the other two methods yield biased estimation. Numerical static error shows that the proposed method yields better maximum error than Davis's. And the three methods yield similar averaged error. Centin's methods achieve best performance on smooth surface filling. Plane extension filling of this type of holes tends to yield relative large residue distortion near the

center of the hole, while the NURBS surface extension often yields better accuracy.

**7.2. Filling of Complex Holes.** In order to examine the performances of the algorithm on filling complex holes, holes with missing curve points (Hole III and Hole IV) or corner points (Hole V) are artificially generated. And then, they are filled by [5, 28] and proposed method.

As shown in Figure 13, Davis's and Centin's methods yield biased estimation for filling of holes with missing feature points, and our proposed method achieves almost ideal recovery without error. Numerical results in Table 3 also validate the accuracy of our proposed method in filling of these types of holes.

As shown in Figure 14, our proposed method performs far better than Davis's and Centin's methods for filling of holes with missing curve points. Numerical results in Table 3 also validate the accuracy of our proposed method in filling of these types of holes.

As shown in Figure 15, our proposed method performs far better than Davis's and Centin's methods for filling of holes with missing corner points. Numerical results in Table 3 also validate the accuracy of our proposed method in filling of these types of holes.

In fact, the complex holes are difficult to be filled through simple plane or fitted surface extension without reliable neighboring segmentation and robust surface fitting. In addition, post-point sampled surface smoothing is often involved for better transition between different surfaces.

**7.3. Accuracy Analysis.** In this subsection, the maximum and averaged errors in filling of hole using three methods are

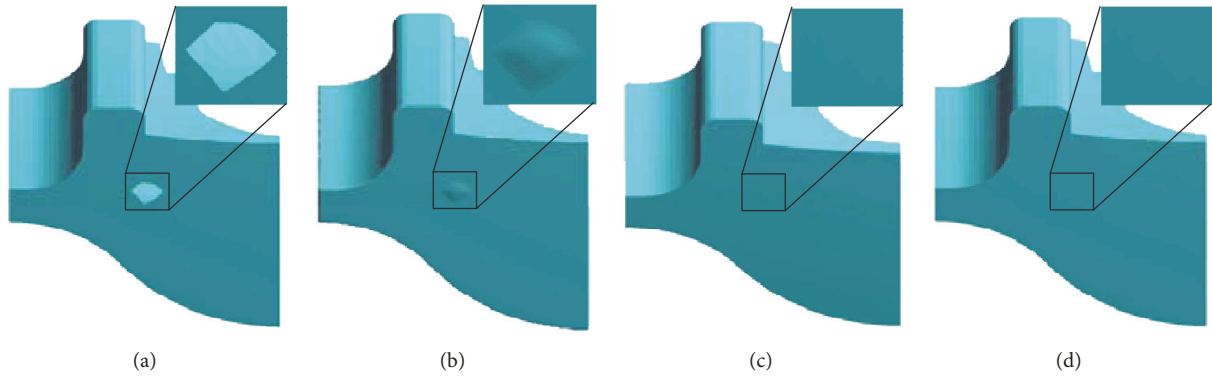


FIGURE 11: Visualization of filled results of Hole I. (a) Hole located on plane. (b) Filling result of Davis et al. (c) Filling result of Centin et al. (d) Proposed result.

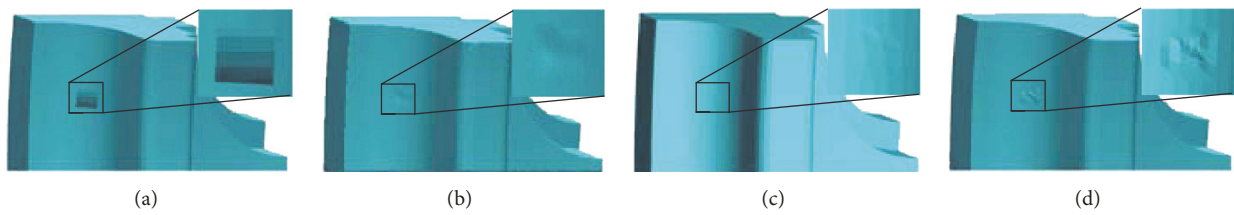


FIGURE 12: Visualization of filled results of Hole II. (a) Hole located on smooth surface. (b) Filling result of Davis et al. (c) Filling result of Centin et al. (d) Proposed result.

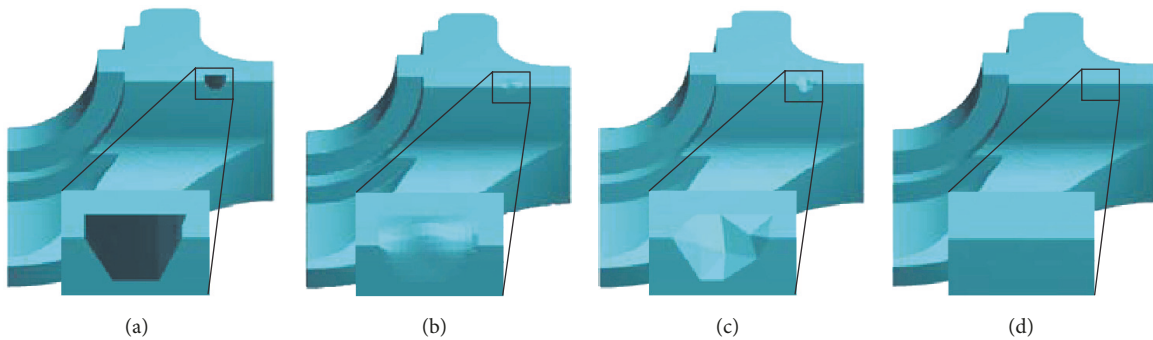


FIGURE 13: Visualization of filled results of Hole III. (a) Hole with sharp feature missing. (b) Filling result of Davis et al. (c) Filling result of Centin et al. (d) Our result.

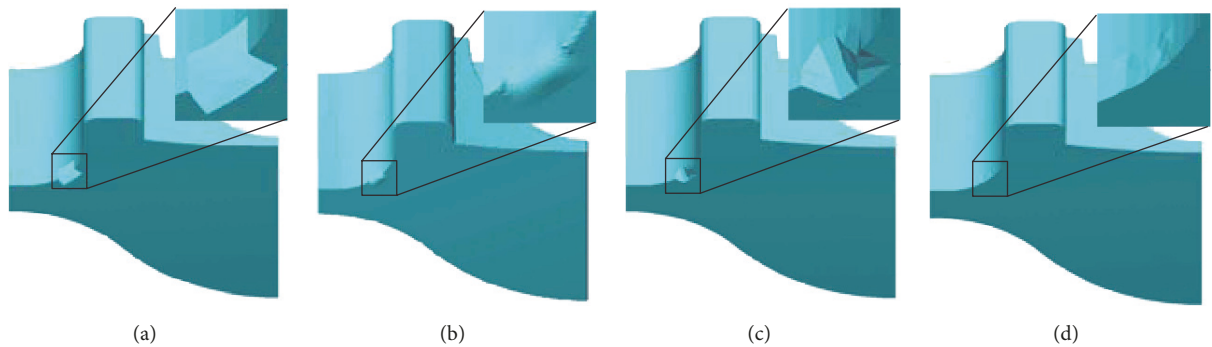


FIGURE 14: Visualization of filled results of Hole IV. (a) Hole with sharp feature missing. (b) Filling result of Davis et al. (c) Filling result of Centin et al. (d) Our result.

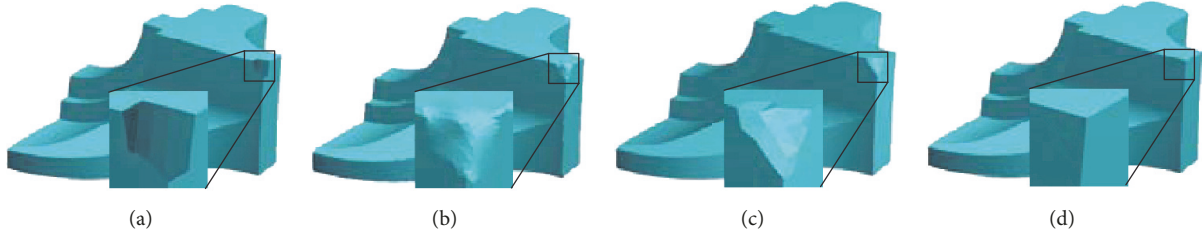


FIGURE 15: Visualization of filled results of hole V. (a) Fandisk with a missing corner. (b) Filling result of Davis et al. (c) Filling result of Centin et al. (d) Our result.

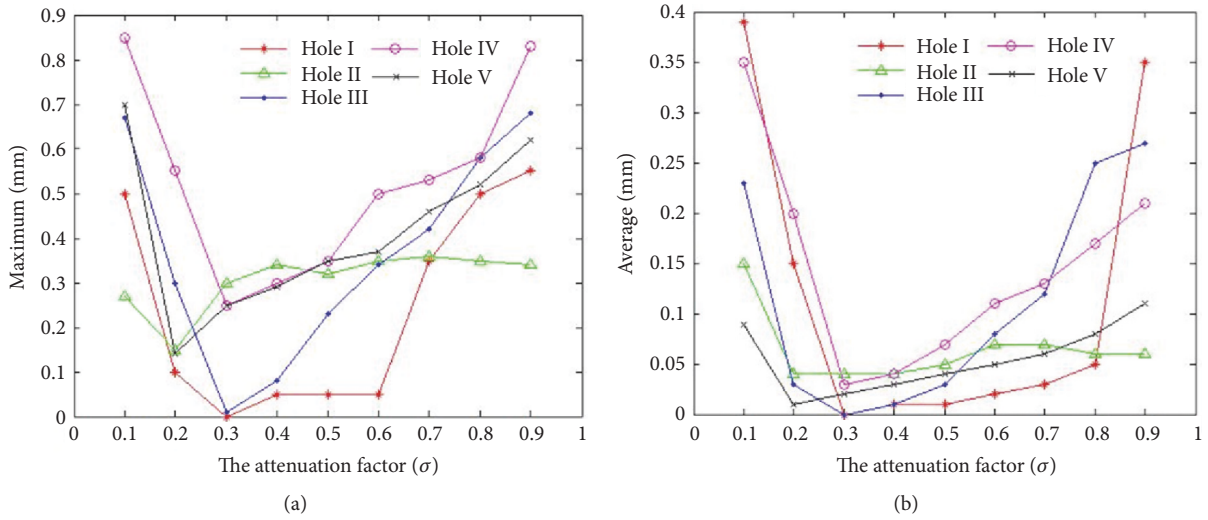


FIGURE 16: Distances comparison between different attenuation factors. (a) Maximum distances. (b) Average distances.

computed and arranged in Table 3. It can be summarized from Table 3 that the proposed hole filling method for point sampled surface yields better accuracy than Centin's and Davis's methods, especially for holes with missing sharp features.

**7.4. Parameter Analysis.** In our method, the scale parameter  $\sigma$  in tensor voting is also a user defined parameter. This parameter influences both the accuracy and the robustness of the algorithm. Thus, experiments with different  $\sigma$  values are performed, and the maximum and averaged error are computed and plotted in Figure 16. In our experiments,  $\sigma$  increase from 0.1 to 0.9. As shown in Figure 16, the algorithm achieves best performance for both maximum and averaged error for  $\sigma \approx 0.25$ . In fact,  $\sigma$  determines the attenuating rate of the energy decay function in tensor voting. Larger  $\sigma$  tends to achieve smoothed but biased estimation. And smaller  $\sigma$  tends to achieve unbiased but noisy estimation.

**7.5. Complexity and Efficiency Analysis.** This paper presented a novel feature preserving hole filling method for point sampled surface, especially on multicriterion based hole boundary identification, spline guided tensor voting based missing

feature point estimation, and plane guided tensor voting based surface point estimation.

The spline guided tensor voting based missing feature point estimation strategy gets rid of either the oversmoothed reconstruction caused by direct spline curve fitting, or the inefficiency of traditional Single Sub-Voxel C Marching. The spline curve provides the most probable estimation for the potential feature point. Then, the tensor voting is used to rectify the estimation in order to achieve a more accurate estimation. Concerning efficiency, the proposed method needs only 4 votes, while the traditional Single Sub-Voxel C Marching needs at least 8 votes (8 vertex of a cube), for one estimation. Furthermore, the traditional Single Sub-Voxel C Marching needs to try multiple cubes for one estimation. Thus, the proposed spline guided tensor voting based missing feature point estimation strategy yields far better efficiency than Single Sub-Voxel C Marching.

The plane guided tensor voting based surface point estimation makes use of plane prediction and tensor voting rectification. Concerning accuracy, the proposed method achieves quadratic estimation for surface point estimation while the traditional Marching Cubes algorithm provides linear estimation. Concerning efficiency, the proposed method

needs 3 votes for each surface point estimation, while the traditional Marching Cubes algorithm needs at least 8 votes.

## 8. Conclusions and Remarks

This paper proposed a new feature preserving hole filling algorithm to point sampled surface. A novel hole multicriterion based boundary identification method for point sampled surface is proposed to improve the reliability of hole boundary point identification. A spline curve guided tensor voting method is proposed to infer the missing feature points. A plane guided tensor voting mechanism is proposed to infer the missing surface points. Experimental results validate the effectiveness and accuracy of our proposed methods in recovering holes on point sampled surface including the sharp features.

In future research, the authors tend to work on adaptive scaling and higher order tensor voting and its application in repairing of higher order data, e.g., simultaneous repairing of texture and geometrical information of 373 textured point cloud.

## Data Availability

The data used to support the findings of this study are available from the corresponding author upon request.

## Conflicts of Interest

The authors declare that they have no conflicts of interest.

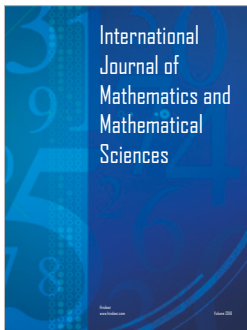
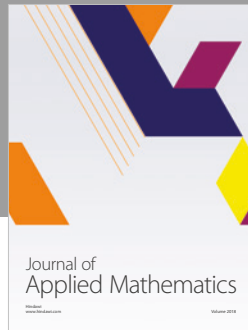
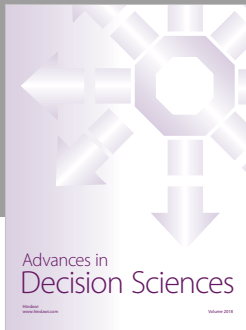
## Acknowledgments

This research was supported by National Natural Science Foundation of China (Grants nos. 51305390 and 61501394) and Natural Science Foundation of HeBei Province (Grant no. F2016203312).

## References

- [1] T. Várady, R. R. Martin, and J. Cox, "Reverse engineering of geometric models—an introduction," *Computer-Aided Design*, vol. 29, no. 4, pp. 255–268, 1997.
- [2] L. Peter, "Filling holes in meshes," in *Proceedings of the Eurographics/acm SIGGRAPH Symposium on Geometry Processing*, pp. 200–205, 2003.
- [3] M. Attene, "A lightweight approach to repairing digitized polygon meshes," *The Visual Computer*, vol. 26, no. 11, pp. 1393–1406, 2010.
- [4] J.-P. Pernot, G. Moraru, and P. Véron, "Filling holes in meshes using a mechanical model to simulate the curvature variation minimization," *Computers and Graphics*, vol. 30, no. 6, pp. 892–902, 2006.
- [5] J. Davis, S. Marschner, M. Garr, and M. Levoy, "Filling holes in complex surfaces using volumetric diffusion," in *Proceedings of the First International Symposium on 3D Data Processing Visualization and Transmission*, pp. 428–861, Padova, Italy.
- [6] T. Ju, "Robust repair of polygonal models," in *Proceedings of the ACM Transactions on Graphics - Proceedings of ACM SIGGRAPH 2004*, pp. 888–895, August 2004.
- [7] L. A. Piegl and W. Tiller, "Filling n-sided regions with NURBS patches," *The Visual Computer*, vol. 15, no. 2, pp. 77–89, 1999.
- [8] G. Xu, Q. Pan, and C. L. Bajaj, "Discrete surface modelling using partial differential equations," *Computer Aided Geometric Design*, vol. 23, no. 2, pp. 125–145, 2006.
- [9] S. Park, X. Guo, H. Shin, and H. Qin, "Surface completion for shape and appearance," *The Visual Computer*, vol. 22, no. 3, pp. 168–180, 2006.
- [10] W. Zhao, S. Gao, and H. Lin, "A robust hole-filling algorithm for triangular mesh," *The Visual Computer*, vol. 23, no. 12, pp. 987–997, 2007.
- [11] A. Sharf, M. Alexa, and D. Cohen-Or, "Context-based surface completion," in *Proceedings of the ACM Transactions on Graphics - Proceedings of ACM SIGGRAPH 2004*, pp. 878–887, August 2004.
- [12] P. Chalmovianský and B. Jüttler, "Filling Holes in Point Clouds," in *Mathematics of Surfaces*, vol. 2768 of *Lecture Notes in Computer Science*, pp. 196–212, Springer Berlin Heidelberg, Berlin, Heidelberg, 2003.
- [13] Hangzhou, "An Algorithm for Automatic Filling of Holes of Point Cloud in Reverse Engineering," *Journal of Computer Aided Design Computer Graphics*, vol. 8, pp. 1793–1797, 2005.
- [14] Y. Jun, "A piecewise hole filling algorithm in reverse engineering," *Computer-Aided Design*, vol. 37, no. 2, pp. 263–270, 2005.
- [15] Z. Li, D. S. Meek, and D. J. Walton, "Polynomial blending in a mesh hole-filling application," *Computer-Aided Design*, vol. 42, no. 4, pp. 340–349, 2010.
- [16] W. Xiaochao, "Automatic hole-filling of CAD models with feature-preserving," *Computers Graphics*, vol. 2, no. 2012, pp. 101–110, 2012.
- [17] L. Hongbin and W. Wei, "Feature preserving holes filling of scattered point cloud based on tensor voting," in *Proceedings of the 2016 IEEE International Conference on Signal and Image Processing, ICSIP 2016*, pp. 402–406, China, August 2016.
- [18] G. Guy and G. Medioni, "Inference of surfaces, 3D curves, and junctions from sparse, noisy, 3D Data," *IEEE Transactions on Pattern Analysis and Machine Intelligence*, vol. 19, no. 11, pp. 1265–1277, 1997.
- [19] P. Mordohai and G. Medioni, "Stereo using monocular cues within the tensor voting framework," *IEEE Transactions on Pattern Analysis and Machine Intelligence*, vol. 28, no. 6, pp. 968–982, 2006.
- [20] L. A. Loss, G. Bebis, and B. Parvin, "Tunable tensor voting for regularizing punctate patterns of membrane-bound protein signals," in *Proceedings of the 2009 IEEE International Symposium on Biomedical Imaging: From Nano to Macro, ISBI 2009*, pp. 1378–1381, USA, July 2009.
- [21] C.-K. Tang and G. Medioni, "Curvature-augmented tensor voting for shape inference from noisy 3D data," *IEEE Transactions on Pattern Analysis and Machine Intelligence*, vol. 24, no. 6, pp. 858–864, 2002.
- [22] J. Jia and C.-K. Tang, "Inference of segmented color and texture description by tensor voting," *IEEE Transactions on Pattern Analysis and Machine Intelligence*, vol. 26, no. 6, pp. 771–786, 2004.
- [23] W.-S. Tong, C.-K. Tang, P. Mordohai, and G. Medioni, "First order augmentation to tensor voting for boundary inference and multiscale analysis in 3D," *IEEE Transactions on Pattern*

- Analysis and Machine Intelligence*, vol. 26, no. 5, pp. 594–611, 2004.
- [24] M. K. Park, S. J. Lee, and K. H. Lee, “Multi-scale tensor voting for feature extraction from unstructured point clouds,” *Graphical Models*, vol. 74, no. 4, pp. 197–208, 2012.
- [25] X. He, Y. Zhuo, and M. Pang, “An algorithm for extracting hole-boundary from point clouds,” *Transactions of the Chinese Society for Agricultural Machinery*, vol. 45, no. 2, pp. 291–296, 2014.
- [26] Y. Jie and ETAL, “The Repair Algorithm of 3D Point Cloud Holes and the Application of The Reconstruction in Plant Forms,” *Journal of Agricultural Mechanization Research*, 2013.
- [27] G. Medioni, M. S. Lee, and C. K. Tang, “A Computational Framework for Segmentation and Grouping. A Computational Framework for Segmentation Grouping,” *A Computational Framework for Segmentation and Grouping*, pp. 243–253, 2000.
- [28] M. Centin and A. Signoroni, “RameshCleaner: conservative fixing of triangular meshes,” *Stag: Smart TOOLS & Apps for Graphics*, 2015.



**Hindawi**

Submit your manuscripts at  
[www.hindawi.com](http://www.hindawi.com)

